Supporting Information

Co-improvement the electrocatalytic performance and H$_2$S tolerance of Sr$_2$Fe$_{1.5}$Mo$_{0.5}$O$_{6-\delta}$

based anode for solid oxide fuel cells

*Chunming Xu,[a] Lihong Zhang,[a] Wang Sun,[*a] Rongzheng Ren,[a]   Xiaoxia Yang ,[a] Minjian Ma,[a] Jinshuo Qiao,[a]*

*Zhenhua Wang,[a]   Shuying Zhen,[b] Kening Sun[*a]*

[a] Beijing Key Laboratory for Chemical Power Source and Green Catalysis, School of Chemistry

and Chemical Engineering, Beijing Institute of Technology, Beijing, 100081, People's Republic

of China.

[b] State Key Laboratory for Advanced Metals and Materials, University of Science and Technology

Beijing, Beijing 100083, China.

Corresponding Author

*Email: sunwang@bit.edu.cn (Wang Sun); bitkeningsun@163.com (Kening Sun)

Oxygen ion transfer properties

Compact SFM and SFMT rectangular bars were prepared for the measurement of conductivity relaxation (ECR). Firstly, the sample powder and PVA(polyvinyl alcohol) binder are evenly mixed by grinding. Then the powder was pressed into a rectangular stainless steel mold at a pressure of 25 MPa. Finally, the sample bars was densified by sintering at 1300 °C for 5 h. Archimedes method was used to measure the density of the sintered sample strip to 98%.

The ECR measurement was performed by an abrupt switch of oxygen partial pressure from 1.07×10^{-20} (a mixture of 95 ml min^{-1} of Ar and 5 ml min^{-1} of H$_2$) to 2.69×10^{-21} (a mixture of 90 ml min^{-1} of Ar and 10 ml min^{-1} of H$_2$) , with a digital multimeter (2400, Keithley) by using the four-point technique. The dense bar samples of SFM and SFMT sample bars for testing are 0.53×0.13×0.23 cm and 0.53×0.12×0.22 cm in size.

The chemical bulk diffusion coefficient (D_{chem}) and surface exchange coefficient (k_{chem}) were obtained by fitting the electrical conductivity relaxation curves with Eq. (S1 and S2).

$$f(t) = \frac{\sigma(t) - \sigma(0)}{\sigma(\infty) - \sigma(0)}$$

(S1)

$$f(t) = 1 - \sum_{m=1}^{\infty}\sum_{n=1}^{\infty}\sum_{l=1}^{\infty} \frac{2L_x^2 exp(\dfrac{-\alpha_m^2 D_{chem}t}{x^2})}{\alpha_m^2(\alpha_m^2 + L_x^2 + L_x)} \times \frac{2L_y^2 exp(\dfrac{-\beta_n^2 D_{chem}t}{y^2})}{\beta_n^2(\beta_n^2 + L_y^2 + L_y)} \times \frac{2L_z^2 exp(\dfrac{-\gamma_l^2 D_{chem}t}{x^2})}{\gamma_m^2(\gamma_l^2 + L_z^2 + L_z)}$$

(S2)

where f (t) refers to the normalized conductivity, while σ (0), σ (t) and σ (∞) represent the initial, time-dependent and final conductivity, respectively. Eq. (S3) presents the calculation process of parameters L_x, L_y and L_z.
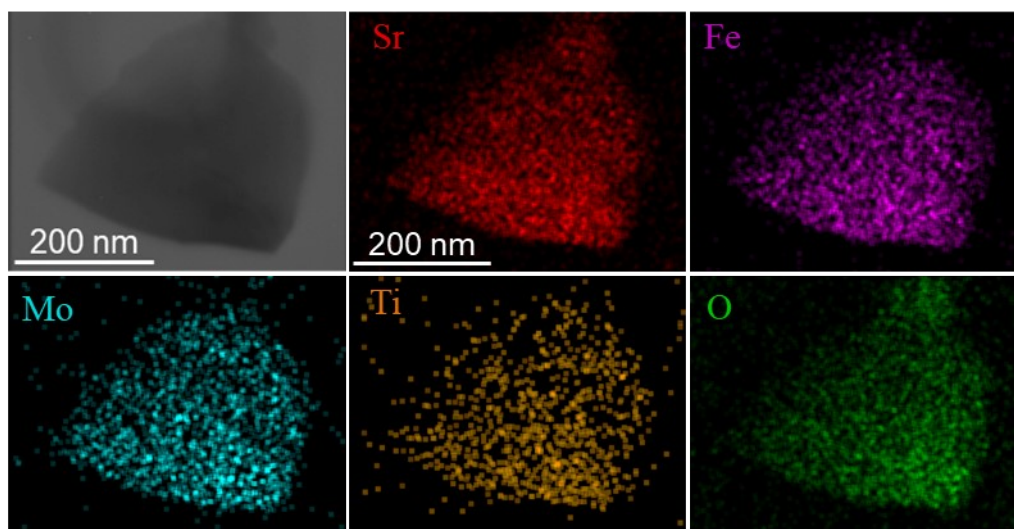
$$L_x = x\frac{k_{chem}}{D_{chem}}, L_y = y\frac{k_{chem}}{D_{chem}}, L_z = z\frac{k_{chem}}{D_{chem}}$$

(S3)

Herein, α_m, β_n and γ_l represent the mth, nth and lth positive root of the transcendental Eq. (S4), respectively.
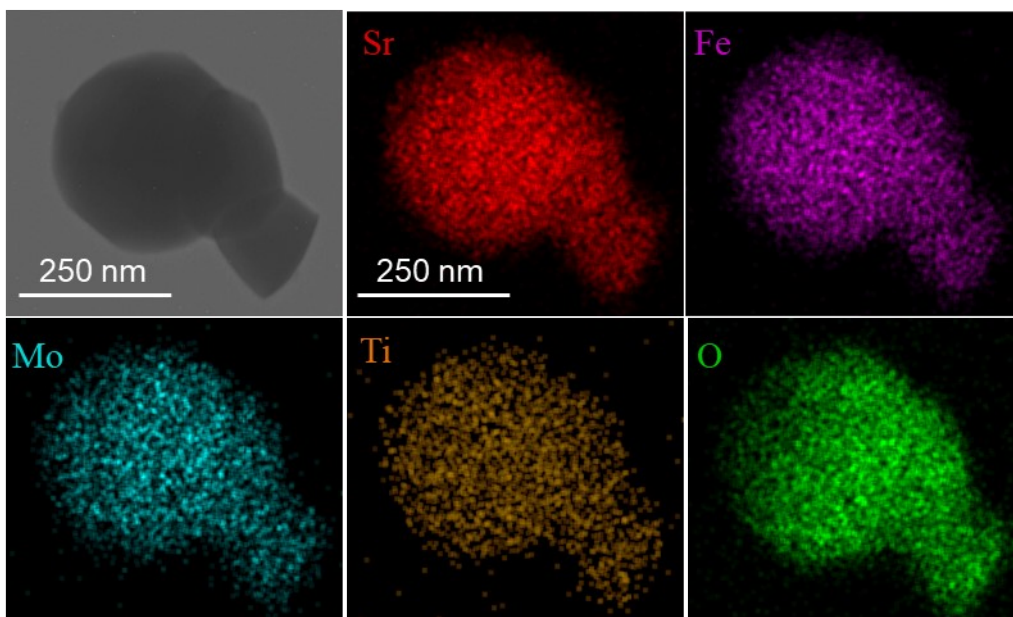
$$\alpha_m \tan\alpha_m = L_x , \beta_n \tan\beta_n = L_y , \gamma_l \tan\gamma_l = L_z$$

(S4)
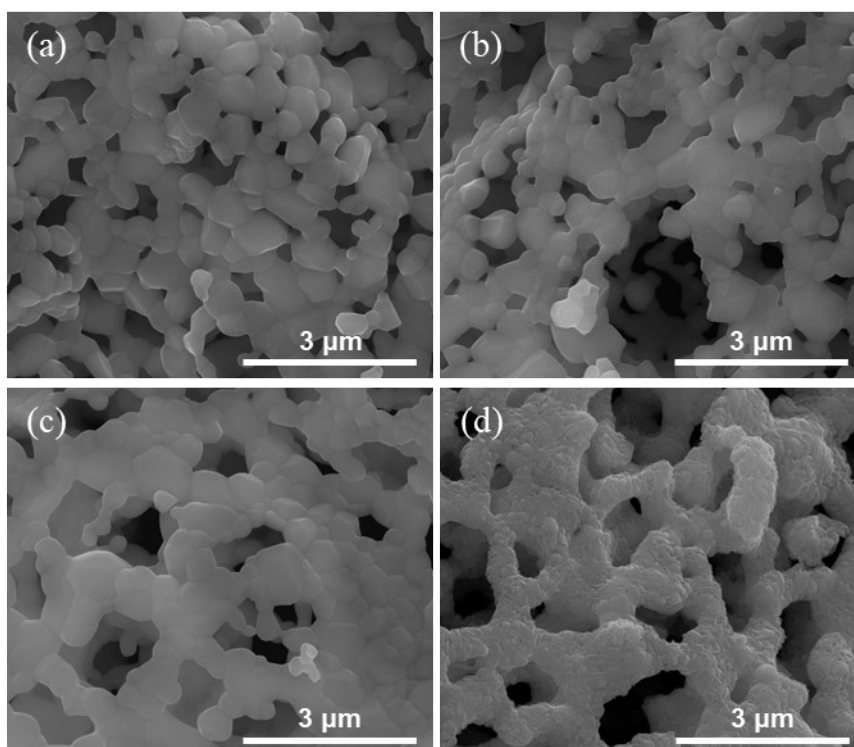
Fig. S1. SEM image of SFMT and SFM samples reduced at different H_2S concentrations (a) SFMT 0 ppm, (b) SFMT 1000 ppm, (c) SFM 0 ppm, (d) SFM 1000 ppm.
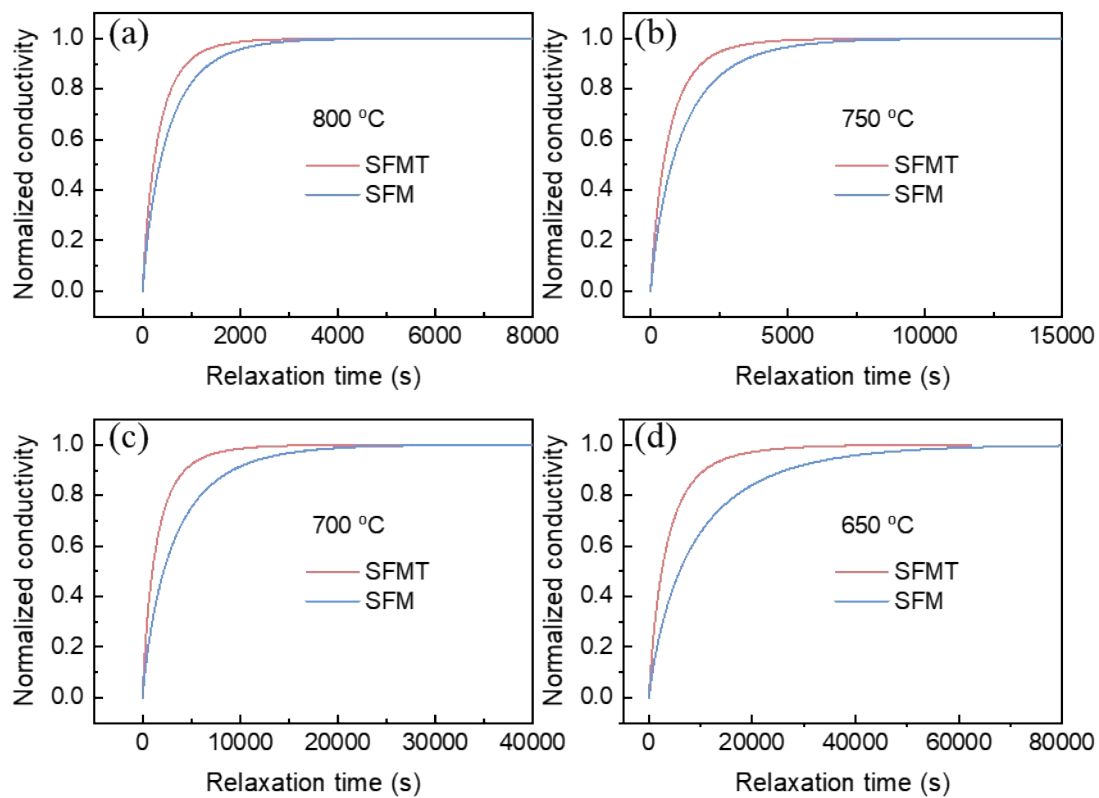

Fig. S2. STEM image and the corresponding EDX elemental mapping traces of the SFMT after reduction at 800 °C in 5% H_2/Ar for 24 h.
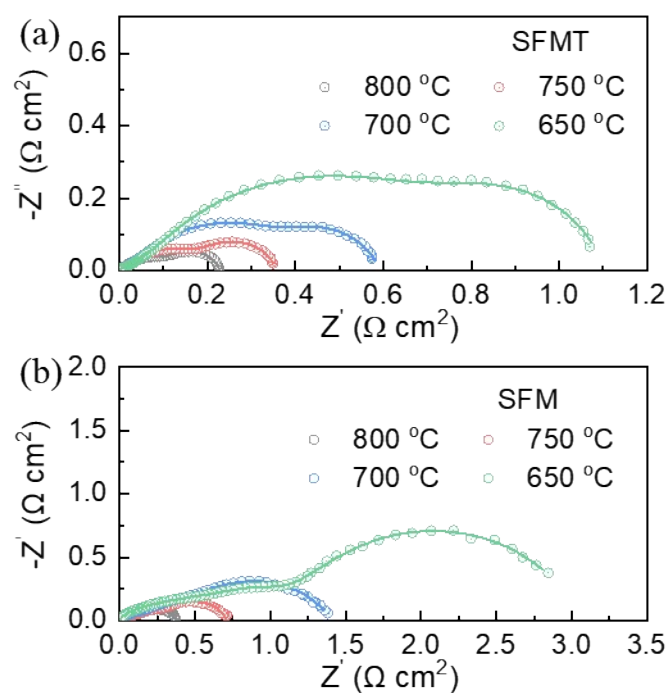
Fig. S3. STEM image and the corresponding EDX elemental mapping traces of the SFMT after reduction at 800 °C in 5% H_2/Ar + 1000 ppm H_2S for 24 h.
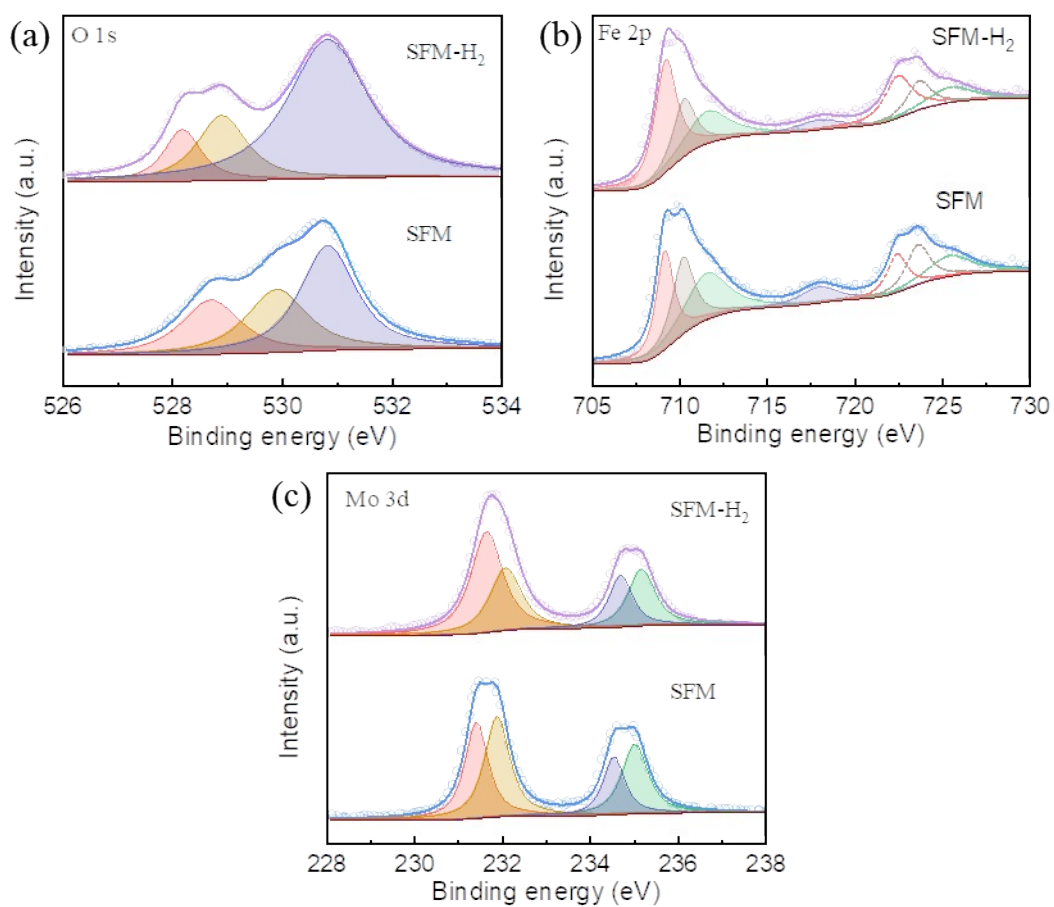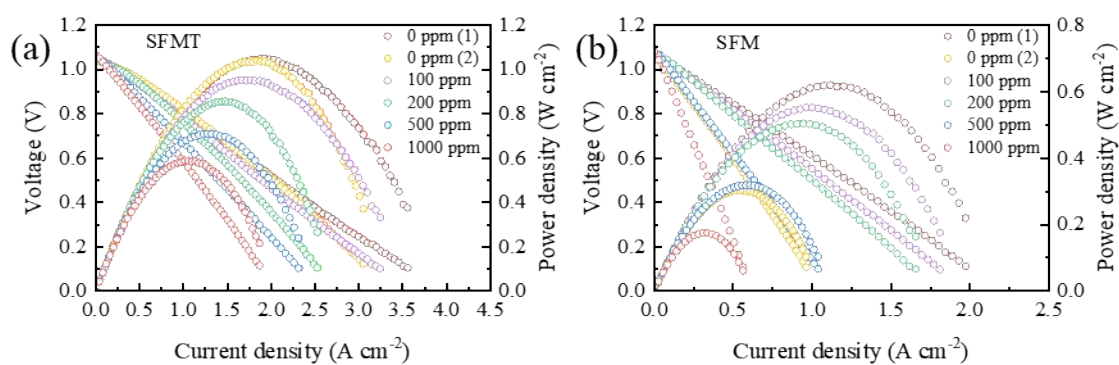

Fig. S4. XPS spectra of SFM and SFM-H_2 (a) O 1s, (b) Fe 2p, (c) Mo 3d.

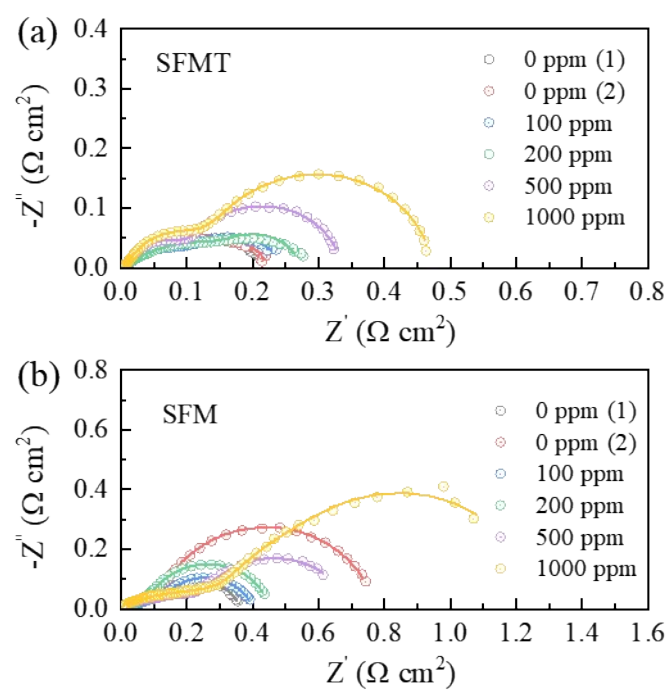**Fig. S5.** Electrical conductivity relaxation curves of SFMT and SFM samples at different temperature, (a) 800 °C, (b) 750 °C, (c) 700 °C, (d) 650 °C.

Fig. S6. The electrochemical impedance spectra measured at various temperatures for

(a) SFMT and (b) SFM electrodes.

Fig. S7. *I-V-P* curves for single cells with (a) SFMT and (b) SFM anodes at 800 °C

under different H_2S concentrations.

Fig. S8. EIS curves of the single cells with (a) SFMT and (b) SFM anodes at 800 °C under different H₂S concentrations.

Table S1. Summary of O valence state in percentage of SFMT and SFM by XPS analysis

Valence State	SFMT		SFM	
	Pristine (%)	Reduced (%)	Pristine (%)	Reduced (%)
O^{2-}	19.5	14.8	25.1	11.7
O_2^{2-}/O^-	27.9	31.2	29.8	19.9
CO_3^{-}/OH^-	46.1	47.2	45.1	68.4
H_2O	6.5	68.2	0	0

Table S2. Summary of Fe valence state in percentage of SFMT and SFM by XPS analysis

Valence State	SFMT		SFM	
	Pristine (%)	Reduced (%)	Pristine (%)	Reduced (%)
Fe^{2+}	31.5	46.4	32.6	47.8
Fe^{3+}	42.0	31.6	33.5	25.5
Fe^{4+}	26.5	22.0	33.9	26.7
Average valence	2.95	2.76	3.01	2.79

Table S3. Summary of Mo valence state in percentage of SFMT and SFM by XPS analysis

Valence State	SFMT		SFM	
	Pristine (%)	Reduced (%)	Pristine (%)	Reduced (%)
Mo^{5+}	44.6	61.3	44.5	55.7
Mo^{6+}	55.4	38.7	55.5	44.3
Average valence	5.55	5.39	5.55	5.44

Table S4 k_{chem} and D_{chem} values of SFMT and SFM materials at different temperatures

Temperature	SFMT		SFM	
	$K_{chem}\times10^4$	$D_{chem}\times10^5$	$K_{chem}\times10^4$	$D_{chem}\times10^5$
(°C)	(cm s^{-1})	(cm^2 s^{-1})	(cm s^{-1})	(cm^2 s^{-1})
800	1.18	3.62	0.78	2.31
750	0.74	2.08	0.38	0.89
700	0.36	0.84	0.16	0.39
650	0.14	0.39	0.055	0.13

Table S5 Interface polarization resistance (Rp) values for the single cell at 800 °C using Fe-based perovskite electrodes reported in the literature

Anodes	Electrolytes	Cathode	Fuels	R_p (Ω cm^2)	Ref
SFM	LSGM(265μm)	SFM	H$_2$	0.46	1
La$_{1.2}$Sr$_{0.8}$Mn$_{0.4}$Fe$_{0.6}$O$_4$-GDC	LSGM(280μm)	LSCF–GDC	H$_2$	0.31	2
Sr$_{1.95}$Fe$_{1.4}$Ni$_{0.1}$Mo$_{0.5}$O$_{6-\delta}$	LSGM(300 μm)	La$_{0.6}$Sr$_{0.4}$Fe$_{0.8}$Co$_{0.2}$O$_{3-\delta}$	H$_2$	0.48	3
La$_{0.5}$Sr$_{0.5}$Fe$_{0.9}$Mo$_{0.03}$Ni$_{0.07}$O$_{3-\delta}$	LSGM(280 μm)	Ba$_{0.5}$Sr$_{0.5}$Co$_{0.9}$Nb$_{0.1}$O$_{3-\delta}$	H$_2$	0.24	4
SFMT	LSGM(300 μm)	LSCF–SDC	H$_2$	0.23	This work

References

1. Q. Liu, X. Dong, G. Xiao, F. Zhao and F. Chen, *Advanced Materials*, 2010, **22**, 5478-5482.
2. Y. S. Chung, T. Kim, T. H. Shin, H. Yoon, S. Park, N. M. Sammes, W. B. Kim and J. S. Chung, *Journal of Materials Chemistry A*, 2017, **5**, 6437-6446.
3. J. Feng, J. Qiao, W. Wang, Z. Wang, W. Sun and K. Sun, *Electrochimica Acta*, 2016, **215**, 592-599.
4. J. Xu, M. Wu, Z. Song, Y. Chen, L. Zhang, L. Wang, H. Cai, X. Su, X. Han, S. Wang and W. Long, *Journal of the European Ceramic Society*, 2021, **41**, 4537-4551.